Structure Development in the Phenolic Resin/Poly(methyl methacrylate-*co*-ethyl acrylate) Copolymer Blends

BONG SUP KIM,[1] GEN-ICHI NAKAMURA,[2] TAKASHI INOUE[2]

[1] R&D Center, Sunkyong Industries Ltd., 600 Jungja 1-Dong, Changan-Ku, Suwon, Kyungki 440-745

[2] Department of Organic and Polymeric Materials, Tokyo Institute of Technology, 1-12-1 Ookayama, Meguro-Ku, Tokyo 152, Japan

Received 30 July 1997; accepted 4 November 1997

ABSTRACT: Single-phase mixtures of phenolic derivatives with three poly(methyl methacrylate-*co*-ethyl acrylate) copolymers [P(MMA-*co*-EA)s] were cured in the presence of hexamethylenetetramine and the reaction kinetics and phase-separation processes during cure were investigated by differential scanning calorimetry (DSC), light scattering, and optical microscopy (OM). DSC measurements revealed that the higher the fraction of multifunctional phenols in the total phenols the lower the conversion at gelation in the phenolic-rich phase. The time variation of the light-scattering profile during cure demonstrated the characteristic feature for spinodal decomposition. OM observation revealed that a cocontinuous two-phase structure appeared after a certain time lag and coarsened to a spherical domain structure consisting of phenolic resin particles dispersed in the P(MMA-*co*-EA)s matrix. The periodic distances, Λ_m, in the phase-separated structure changed with curing time: (1) The higher the component of MMA in P(MMA-*co*-EA)s and (2) the higher the fraction of multifunctional phenols in the total phenols, the smaller the Λ_m. These results may imply that the phase separation is suppressed by the faster gelation in the phenolic-rich phase so that the phase-separated structure can be fixed by the network formation in the phenolic-rich phase at the early stage of spinodal decomposition. This results in a two-phase structure with a shorter periodic distance. © 1998 John Wiley & Sons, Inc. J Appl Polym Sci 68: 1829–1837, 1998

Key words: phenolic; poly(methyl methacrylate-*co*-ethyl acrylate); conversion; gelation; phase separation

INTRODUCTION

The use of thermoset polymers in many applications is extensive. One of the most important thermoset polymers is phenolic resin, which has many desirable properties, such as high modulus, high strength, excellent chemical resistance, and good dimensional stability. Consequently, it is widely used for many important applications, for example, in structural adhesives, as an insulating material for electric and electronic components, and in reinforced plastics and matrix resins for advanced composite materials.[1–3] However, it is inherently brittle due to its higher crosslink density and, consequently, has limited use in applications requiring high impact fracture strength. This problem can be moderated by incorporating the elastomeric and/or thermoplastic polymers into phenolics. So far, various attempts to enhance the impact strength of thermosetting resins by modification with elastomeric and/or thermoplastic polymers have been reported in the literature.

Correspondence to: B. S. Kim.

Journal of Applied Polymer Science, Vol. 68, 1829–1837 (1998)
 CCC 0021-8995/98/111829-09

However, most studies have focused on epoxy resins.[4–10] Also, very limited information has been reported on the structure development and impact strength enhancement for phenolic resins. Shu and Konii[11] developed a modified phenolic resin in which some portion of the phenolic hydroxyl groups was reacted with alkyl titanate and the modified phenolic resin was cured by hexamethylenetetramine. Culbertson et al.[12] studied the modification of phenolic resin which was cured by phenylene–bisoxazoline. Matsumoto et al.[13] reported that the modification of phenolic resin by a *p*-hydroxyphenylmaleimide/acrylic ester copolymer improves both flexural strength and heat resistance.

In our previous article,[14] we investigated the effect of the crosslinking density of phenolic resins and the molecular weight of poly(methyl methacrylate) (PMMA) on the miscibility and structure development of a phenolic derivative/PMMA mixture during cure.

In this article, we employed the mixtures of phenolic derivatives with three poly(methyl methacrylate-*co*-ethyl acrylate) copolymers [P(MMA-*co*-EA)s] and studied the reaction kinetics by DSC, the phase separation process by light scattering, and the morphological development by optical microscopy to investigate the effect of various MMA/EA compositions of P(MMA-*co*-EA)s and the fraction of multifunctional phenol in total phenols on the structure development in phenolic/P(MMA-*co*-EA) mixtures.

EXPERIMENTAL

Bisphenol A (BPA; MW = 228 g mol^{-1}) was supplied by Wako Chemical Co. *m*-Phenylphenol (MPP; MW = 170 g mol^{-1}), *o*-phenylphenol (OPP; MW = 200 g mol^{-1}), and *p*-nonylphenol (PNP; MW = 220 g mol^{-1}) were supplied by Tokyo Kasei Chemical Co. (Tokyo, Japan). The curing agent was hexamethylenetetramine (Hexa). Three poly(methyl methacrylate-*co*-ethyl acrylate) copolymers [P(MMA-*co*-EA)s] were synthesized in our laboratory. Their MMA/EA compositions were 100/0, 63/37, and 19/81 wt %. Their glass transition temperatures and number-average molecular weights are 105, 38, and −4°C, and 100K, 150K, and 110K g mol^{-1}, respectively. The structural formulas of the materials employed are shown below:

Phenolic resins

BPA

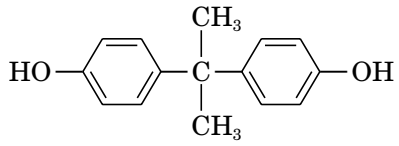

MPP

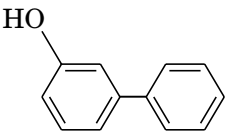

OPP

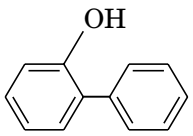

PNP

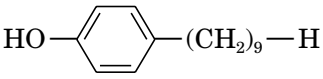

Curing agent

Hexa

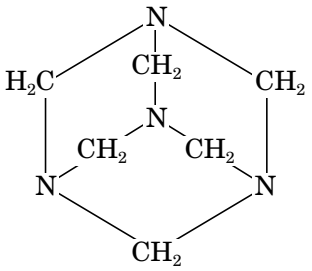

Modifier

P(MMA-*co*-EA)

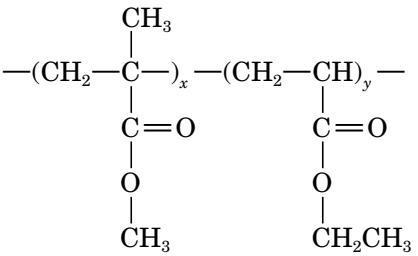

Three P(MMA-*co*-EA)s were prepared by bulk polymerization of the methyl methacrylate monomer (MMA) and the ethyl acrylate monomer (EA) with azobisisobutylonitrile (AIBN). At first, MMA and EA was mixed at ratios of 100/0, 63/37, and 19/81 wt %. Then, AIBN (0.1 wt %) was added to the MMA/EA mixture. After thorough mixing, the mixture was sealed and polymerized at 70°C for 5 h. The glass transition temperatures of the P(MMA-*co*-EA)s obtained were measured by DSC and were 105, 38, and −4°C.

On the other hand, poly(*o*-phenylphenol) (POPP)

was also prepared by bulk polymerization of *o*-phenylphenol (OPP). At first, OPP (35 mmol) and Hexa (23 mmol) were added to a glass tube and the mixture was preheated to 160°C. After thorough mixing, the mixture was sealed and polymerized at 180°C for 5 h and further polymerization was performed at 220°C for 2 h. The molecular weight of the POPP obtained was measured by gel permeation chromatography and was 5900 g mol^{-1}.

The desired amounts of POPP and the three P(MMA-*co*-EA)s were dissolved in acetone at 10 wt % of the total polymer. The solution was cast onto a cover glass (for microscopy). The cast film was further dried under a vacuum of 10^{-4} mmHg for 12 h. The mixture specimens thus obtained were transparent over all compositions and no phase-separated morphology was detected under the optical microscopic observation. Also, the specimen was inserted into a heating stage for the cloud-point measurements. Upon annealing the film at a certain temperature, we observed the onset of phase separation under the light microscope. Based on this observation, we obtained the phase diagrams of the POPP/P(MMA-*co*-EA) mixtures.

We also prepared in the same way the solution-cast specimens of the (BPA + PNP)/Hexa/P(MMA-*co*-EA), (BPA + OPP)/Hexa/P(MMA-*co*-EA), and (MPP + OPP)/Hexa/P(MMA-*co*-EA) mixtures with various MMA/EA compositions. These mixtures also are homogeneous as prepared. The film specimens cast onto a cover glass were inserted into the heating stage of the light-scattering apparatus whose schematic diagram is given in Figure 1 and were allowed to experience isothermal heating. Radiation from a He—Ne gas laser (wavelength 632.8 nm) was applied vertically to the film. The intensity of scattered light from the film was measured under an optical alignment with parallel polarization (Vv). The angular distribution of the scattered light intensity was detected by a one-dimensional photometer with a 46 photodiode array (HASC Co. Ltd). The scattering profiles in a time of 1/30 s were recorded at the appropriate intervals during the isothermal annealing (curing) and were stored in a Forth Engine computer for the analysis. The scattering angle θ within the specimen is related to the observed scattering angle, θ_{obs}, by

$$n \sin \theta = \sin \theta_{obs}$$

where n is the refractive index of the specimen.

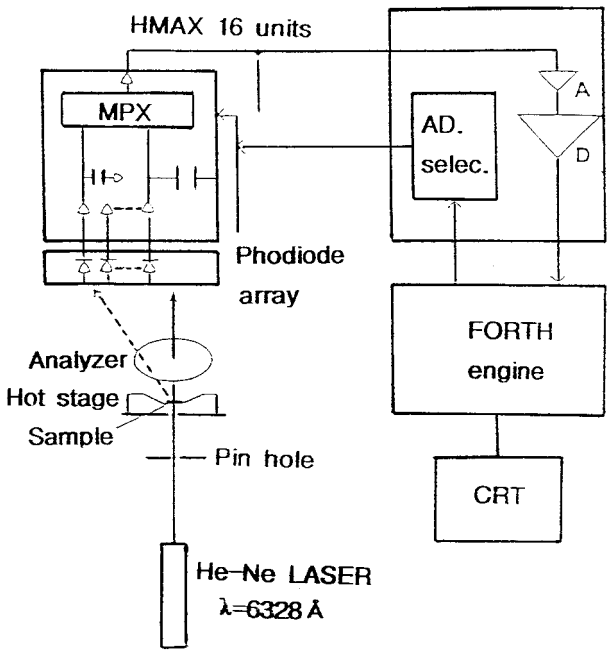

Figure 1 Light-scattering apparatus.

The intensity of the scattered light was corrected by multiplying Cn:

$$Cn = n^2 \cos \theta / (1 - n^2 \sin \theta)^{1/2}$$

A light-scattering pattern was also observed by using a photographic technique.[15]

The kinetics of the curing reaction was examined by DSC (DuPont, Model 910). The heat of the reaction for the uncured mixture was determined from the DSC run at a heating rate of 10°C min^{-1} over the temperature range of 100–350°C. The heat of the reaction occurring during the isothermal curing was obtained by measuring, using the same procedure as above, the heat of the reaction for the already-cured mixture and substracting it from that of the cured one. Therefore, the conversion (i.e., degree of reaction) of the cured mixture up to a given reaction time was estimated by comparing the areas under the exotherm peaks and is given by the following equation:

$$\text{Conversion } (\%) = (1 - A_t/A_0) \times 100$$

where A_0 is the area of an exotherm peak of the uncured material and A_t is that of the cured one. A theoretical conversion at the gelation point was calculated using the Flory–Stockmayer's gelation theory.[16–18]

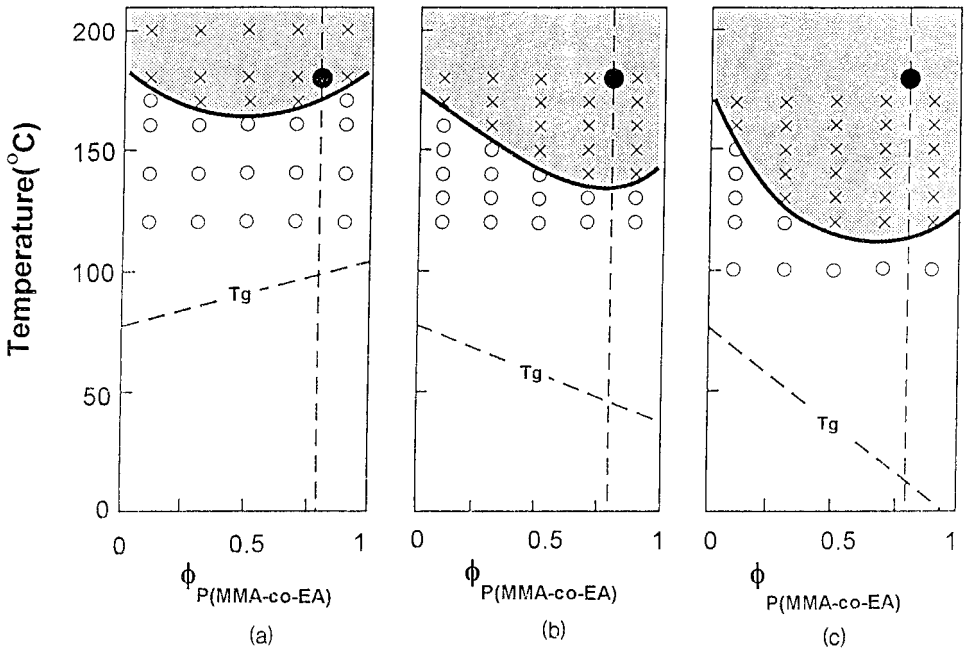

Figure 2 Phase diagrams of POPP/three P(MMA-*co*-EA) mixtures: (a) MMA/EA = 100/0 (wt %); (b) 63/37; (c) 19/81.

RESULTS AND DISCUSSION

Phase Diagram of POPP/P(MMA-*co*-EA)s Mixtures

Figure 2 shows phase diagrams of POPP/three P(MMA-*co*-EA) mixtures with various MMA/EA compositions. The POPP/P(MMA-*co*-EA) mixtures have a lower critical solution temperature (LCST)-type phase behavior as shown in Figure 2(a–c). The LCST of a POPP blend with P(MMA-*co*-EA) having a ratio of MMA 19 to EA81 wt % [P(MMA19-*co*-EA81)] is lower than that with P(MMA-*co*-EA) having a ratio of MMA 100 to EA0 wt % [P(MMA100-*co*-EA0)]. The T_g's of the POPP/P(MMA-*co*-EA) mixtures, estimated by the Fox equation using the T_g data of neat POPP and P(MMA-*co*-EA)s which were measured by DSC, are also shown in Figure 2.

Upon our current understanding of polymer–polymer miscibility, the LCST is expected to decrease as the molecular weight of a thermosetting resin, that is, POPP in our case, increases with curing and then the two-phase region would prevail in the phase diagram with curing of POPP. The T_g of the mixture would be elevated when the molecular weight of POPP increases. These situations are demonstrated schematically in Figure 3. Figure 3 implies that the mixture with composition ϕ is initially at a single phase at an isothermal curing temperature, T_{cure}; however, the system will be thrust into a two-phase region as the curing reaction proceeds. Hence, the spinodal decomposition is expected to take place in the curing process.

Structure Developments of (BPA + PNP)/Hexa/P(MMA-*co*-EA) Mixtures by Light Scattering

An as-cast film of (BPA + PNP)/Hexa/P(MMA100-*co*-EA0) [(1.6 + 14.4)/4/80 wt %] mixture was a homogeneously mixed single-phase system and no appreciable light scattering was detected from the mixture in the very early stages of isothermal curing at 180°C. After some induction period, a ring pattern of light scattering appeared. The ring pattern implies that with curing a regularly phase-separated structure was developed in the mixture. The ring pattern became brighter and its diameter decreased with curing time. A typical example of the change in the light-scattering profile is presented in Figure 4. The characteristic changes of the scattering profile shown in Figure 4 are the hallmarks of spinodal decomposition. However, no appreciable light scattering was detected from a (BPA + PNP)/Hexa/P(MMA100-*co*-EA0) [(16 + 0)/4/80 wt %] mixture when cured at the same T_{cure}. These results can be interpreted in terms of different rates of phase separation and cure reaction between the two mixtures as follows: For

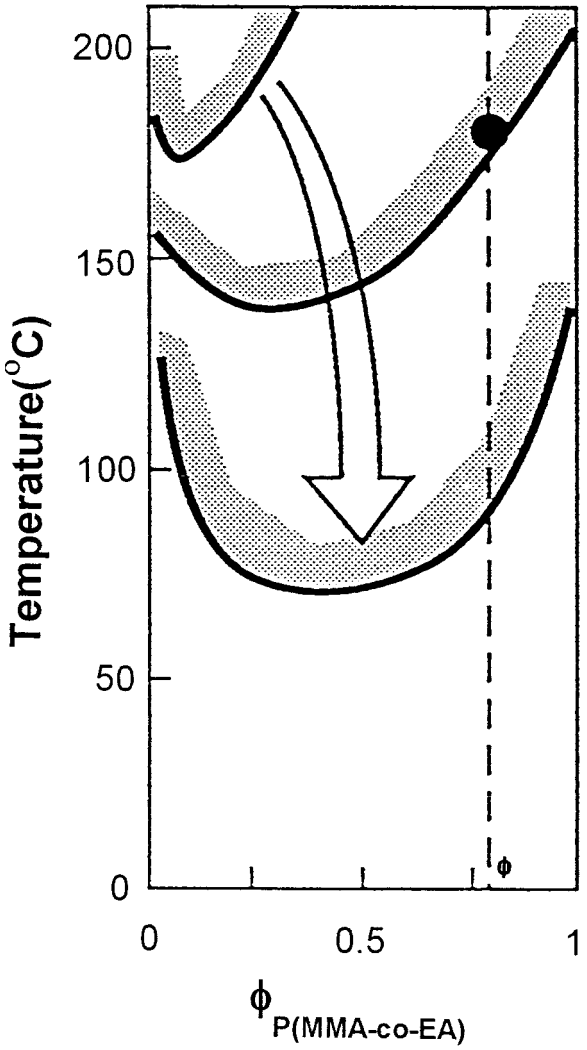

Figure 3 Schematic representation of the variation of phase diagram and T_g with curing in the case of Figure 2(a).

a thermoset/thermoplastic blend, the phase separation is suppressed by the network formation of the thermoset. On the other hand, the molecular weight of a thermoset increases with curing and the phase separation is promoted. Therefore, the final morphology of a thermoset/thermoplastic blend is governed by the competition between these two effects. The reaction rate of the (BPA + PNP)/Hexa/P(MMA100-*co*-EA0) [(16 + 0)/4/80 wt %] mixture is much faster than that of the (BPA + PNP)/Hexa/P(MMA100-*co*-EA0) [(1.6 + 14.4)/4/80 wt %] mixture. Therefore, the phase separation was suppressed by the network formation of a phenolic-rich phase and no phase separation was observed for the (BPA + PNP)/Hexa/P(MMA100-*co*-EA0) [(16 + 0)/4/80 wt %] mixture. But the reaction rate of the (BPA + PNP)/Hexa/P(MMA100-*co*-EA0) [(1.6 + 14.4)/4/80 wt %] mixture was relatively slow and the phase separation progressed until the gelation in the phenolic-rich phase took place. On the other hand, similar results were obtained for the (BPA + OPP)/Hexa/P(MMA100-*co*-EA0) [(3.2 + 12.8)/4/80 wt %)] mixture. We discuss this matter later in more detail.

To discuss a domain spacing of a phase-separated structure, we estimated the periodic distance, Λ_m, in the phase-separated structure as a Bragg's spacing from the peak angle, θ_m, of the scattering profiles in Figure 4. Λ_m is given by

$$\Lambda_m = 2\pi/q, \quad q = (4\pi/\lambda)\sin(\theta_m/2)$$

Therefore,

$$\Lambda_m = \lambda/2n \sin(\theta_m/2)$$

where q is the scattering vector; λ, the wavelength of incident light in the medium; and n, the refractive index. The time variation of Λ_m in the (BPA + PNP)/Hexa/P(MMA-*co*-EA) [(1.6 + 14.4)/4/80 wt %] mixtures during cure at 180°C is plotted in Figures 5 and 6. The Λ_m increases with curing time, indicating a structure coarsening, and then levels off due to the network formation in a phenolic-rich phase. The higher the component of EA in P(MMA-*co*-EA) and the lower the fraction of multifunctional phenols in total phenols, the larger the Λ_m and the higher the slope of the growth rate in the phase-separated structure. On the other hand, the effect of MPP/OPP composition on the Λ_m and conversion at gelation in the (MPP + OPP)/Hexa/P(MMA19-*co*-EA81) mixtures is shown in Table I. As can be seen in the table, the higher the fraction of multifunctional phenols in the total phenols (i.e., the higher crosslinking density), the shorter the Λ_m.

Cure Kinetics

Figure 7 shows the time–conversion curves of (BPA + PNP)/Hexa/P(MMA-*co*-EA)s [(1.6 + 14.4)/4/80 wt %] during cure at 180°C. As expected, the reaction rate increased with increasing the EA component of P(MMA-*co*-EA). The acceleration may be caused by an increased mobility due to the loading of the low T_g component (EA) so that it becomes more significant for the P(MMA19-*co*-EA81) system. To investigate the effect of the fraction of

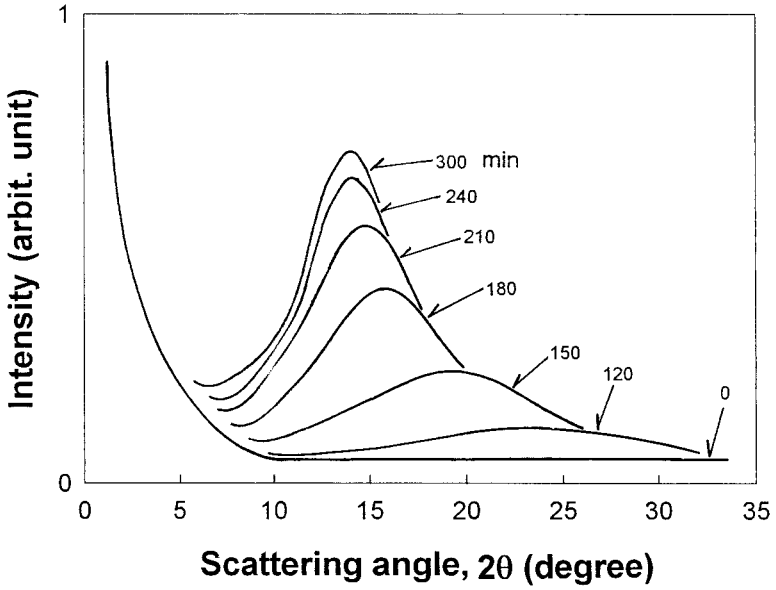

Figure 4 Change in the light scattering profile of the (BPA + PNP)/Hexa/P(MMA63-*co*-EA37) [(13.2 + 12.8)/4/80 wt %] mixture with curing at 180°C. The numbers shown are the cure times.

multifunctional phenols in the total phenols on the reaction rate, we employed a various phenolic derivative mixtures of BPA + PNP, BPA + OPP, and MPP + OPP. The reaction rate of the (MPP + OPP)/Hexa/P(MMA-*co*-EA) mixture is slower than that of the (BPA + OPP)/Hexa/P(MMA-*co*-EA) mixture. It may be caused by a low reactivity due to the lower fraction of multifunctional phenols in the total phenols. According to the Flory–Stockmayer's gelation theory, the conversion at the gelation point decreases with increasing the functionalities of the reactants. For the system containing a mixture of BPA, MPP, PNP, and OPP with functionalities of 4, 3, 2, and 2, respectively, and Hexa, in which Hexa can only react with the phenolic monomer, the critical extent of the reaction at the gel point (Pc) is given by

$$Pc^2 = r/[(f_{\text{phenol}} - 1)(g_{\text{Hexa}} - 1)]$$

where r is the mol ratio of the reacting groups,

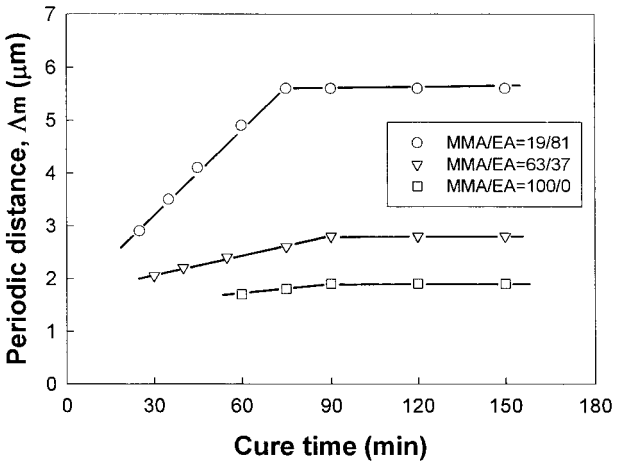

Figure 5 Time variation of Λ_m in the (BPA + PNP)/Hexa/P(MMA-*co*-EA) [(1.6 + 14.4)/4/80 wt %] mixtures during cure at 180°C.

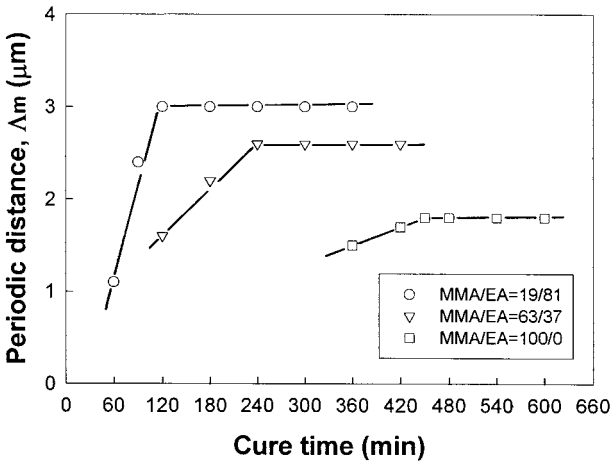

Figure 6 Time variation of Λ_m in the (BPA + PNP)/Hexa/P(MMA-*co*-EA) [(3.2 + 12.8)/4/80 wt %] mixtures during cure at 180°C.

Table I Effect of MPP/OPP Composition on the Λ_m and Conversion at Gelation in (MPP + OPP)/Hexa/P(MMA19-*co*-EA81) Blends Cured at 180°C

MPP/OPP	Conversion (%) at Gelation	Λ_m (μm)
1/9	95.3	3.6
2/8	91.3	2.8
5/5	81.6	1.8
10/0	70.7	—

that is, the mol ratio of phenolics to Hexa, and f_{phenol} and g_{Hexa} are the functionalities of the phenolic resin and Hexa, respectively. Let us calculate the *Pc* for the following cases:

(a) For the mol ratio of (BPA + OPP)/Hexa = (1.0 + 0)/1,

$$Pc^2 = r/[(f_{\text{phenol}} - 1)(g_{\text{Hexa}} - 1)],$$

$$\text{then } Pc = 0.577$$

$$Xn = f + 2/(1 - 2Pc)f + 2 = 4.33$$

(b) For the mol ratio of (BPA + OPP)/Hexa = (0.2 + 0.8)/1

$$rPc^2\rho/[1 - rPc^2(1 - \rho)] = r/$$

$$[(f_{\text{phenol}} - 1)(g_{\text{Hexa}} - 1)], \quad \text{then } Pc = 0.845$$

$$Xn = [f(1 - \rho + 1/r) + 2\rho]/$$

$$[(f(1 - \rho + 1/r - 2Pc) + 2\rho] = 9.05$$

(c) For the mol ratio of (BPA + OPP)/Hexa = (0.1 + 0.9)/1,

$$rPc^2\rho[1 - rPc^2(1 - \rho)]^{-1} = r/$$

$$[(f_{\text{phenol}} - 1)(g_{\text{Hexa}} - 1)], \quad \text{then } Pc = 0.913$$

$$Xn = [f(1 - \rho + 1/r) + 2\rho]/$$

$$[(f(1 - \rho + 1/r - 2Pc) + 2\rho] = 15.73$$

(d) For the mol ratio of (MPP + OPP)/Hexa = (0.1 + 0.9)/1,

$$rPc^2\rho[1 - rPc^2(1 - \rho)]^{-1} = r/$$

$$[(f_{\text{phenol}} - 1)(g_{\text{Hexa}} - 1)], \quad \text{then } Pc = 0.953$$

$$Xn = [f(1 - \rho + 1/r) + 2\rho]/$$

$$[(f(1 - \rho + 1/r - 2Pc) + 2\rho] = 30.21$$

where ρ and $1 - \rho$ are the fractions of BPA and OPP and of MPP and OPP, respectively. *Xn* is the degree of polymerization at gelation. Hence, the theoretical conversion at gelation for the (BPA + OPP)/Hexa = (1.0 + 0)/1, (BPA + OPP) = (0.1 + 0.9)/1, (BPA + OPP)/Hexa = (0.2 + 0.8)/1, and (MPP + OPP)/Hexa = (0.1 + 0.9)/1 mixtures are 0.577, 0.845, 0.913, and 0.953, respectively. The *Xn* for the (BPA + OPP)/Hexa = (1.0 + 0)/1, (BPA + OPP) = (0.1 + 0.9)/1, (BPA + OPP)/Hexa = (0.2 + 0.8)/1, and (MPP + OPP)/Hexa = (0.1 + 0.9)/1 mixtures are 4.33, 9.05, 15.73, and 30.21, respectively. This means that the higher the fraction of multifunctional phenolic, BPA and MPP, in the total phenols, the smaller the value of *Pc* and the higher the value of *Xn*.

On the other hand, we also found an interesting phenomenon in this system as discussed in a previous article,[14] that is, the graft reaction could have taken place between the P(MMA-*co*-EA)s and the phenolic resins. The mechanism of the graft reaction was already described in a previous article.[14]

Morphology Observation by Optical Microscopy

Under the microscope, the as-cast transparent specimen of the (BPA + OPP)/Hexa/P(MMA-*co*-EA) mixtures remained the same for some period of time after a temperature jump from room temperature to the curing temperature. After a certain time lag, a two-phase structure with low contrast appeared and the contrast became higher with further curing. Figure 8(a,b), shows optical

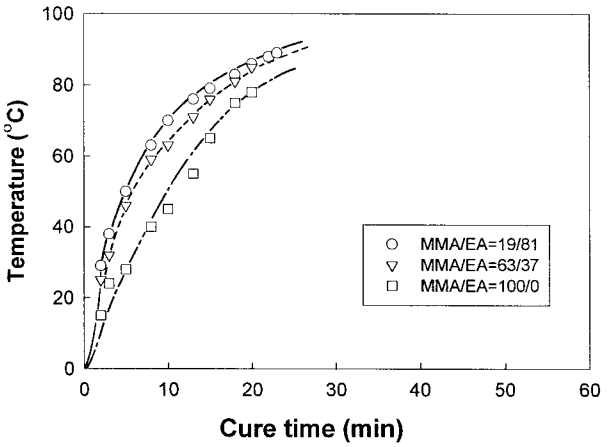

Figure 7 The time–conversion curves of the (BPA + PNP)/Hexa/P(MMA-*co*-EA) [(1.6 + 14.4)/4/80 wt %] mixtures during cure at 180°C.

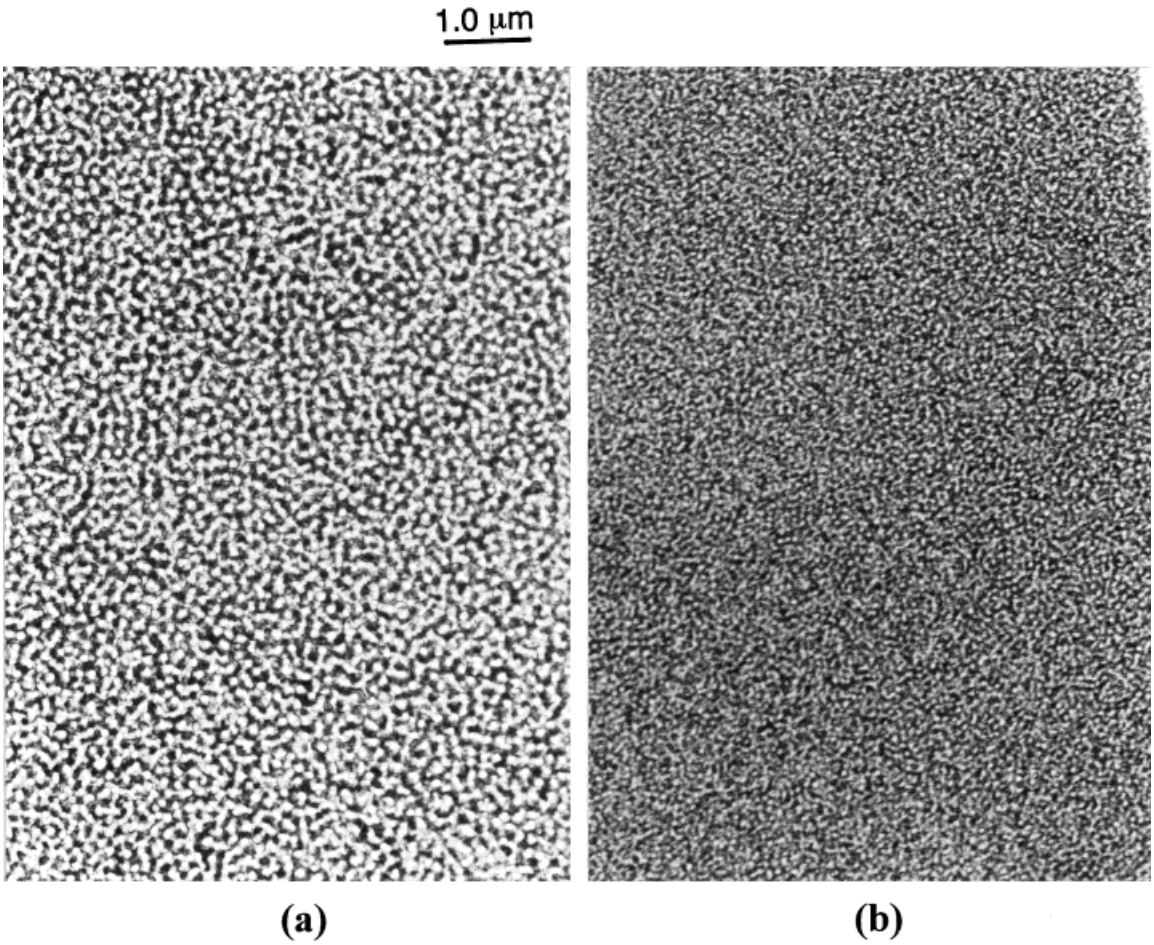

Figure 8 Optical micrographs of (a) (BPA + OPP)/Hexa/P(MMA63-*co*-EA37) [(1.6 + 14.4)/4/80 wt %] and (b) (BPA + OPP)/Hexa/P(MMA63-*co*-EA37) [(8 + 8)/4/80 wt %] mixtures cured at 180°C.

micrographs of the (BPA + OPP)/Hexa/P(MMA63-*co*-EA37) [(1.6 + 14.4)/4/80 wt %] and (BPA + OPP)/Hexa/P(MMA63-*co*-EA37)[(8 + 8)/4/80 wt %] mixtures cured at 180°C. The micrographs clearly show the regular interdomain spacing and uniform domain size distribution and this regularly phase-separated structure is quite similar to the usual spinodal decomposition pattern. The periodic distance in the phase-separated structure of (BPA + OPP)/Hexa/P(MMA-*co*-EA) [(14.4 + 1.6)/4/80 wt %] mixture is smaller than that of the (BPA + OPP)/Hexa/P(MMA-*co*-EA) [(8 + 8)/4/80 wt %] mixture. It may be caused by the beginning of gelation at low conversion due to the higher fraction of multifunctional phenolic in the total phenols. The conversion at gelation of the (BPA + OPP)/Hexa/P(MMA63-*co*-EA37) [1.6 + 14.4)/4/80 wt %] and (BPA + OPP)/Hexa/P(MMA63-*co*-EA37) [(8 + 8)/4/80 wt %] mixtures during cure at 180°C were 0.913 and 0.598, respectively, that is, the phase separation is suppressed by the faster gelation in the phenolic-rich phase so that the phase-separated structure can be fixed by the network formation in the phenolic-rich phase at the early stage of spinodal decomposition. This results in a two-phase structure with a shorter periodic distance. The phase-separated structure became spherical in shape at the late stage of curing. It is consistent with the light-scattering profiles presented in Figure 4.

CONCLUSIONS

Single-phase mixtures of phenolic derivatives with three P(MMA-EA)s were cured in the presence of hexamethylenetetramine and the reaction kinetics and phase-separation processes during

cure were investigated by DSC, light scattering, and optical microscopy (OM). DSC measurements revealed that the higher the fraction of multifunctional phenols in the total phenols, the faster the conversion at gelation in the phenolic-rich phase. The time variation of the light-scattering profile during cure demonstrated the characteristic features for spinodal decomposition. OM observation revealed that a cocontinuous two-phase structure appeared after a certain time lag and coarsened to a spherical domain structure consisting of phenolic resin particles dispersed in the P(MMA-*co*-EA) matrix. The periodic distances in the phase-separated structure changed with curing time: (1) The higher the component of MMA in P(MMA-*co*-EA)s and (2) the higher the fraction of multifunctional phenols in the total phenols, the smaller the periodic distance.

REFERENCES

1. N. J. L. Megson, *Phenolic Resin Chemistry,* Butterworth Press, London, 1958.
2. A. Knop and W. Scheib, *Chemistry and Application of Phenolic Resins,* Springer-Verlag, New York, 1979.
3. A. Tanaka and R. Nakatsuka, *J. Adhes. Soc. Jpn.,* **1,** 97 (1980).
4. C. B. Bucknall and I. K. Patridge, *Polymer,* **24,** 639 (1983).
5. R. S. Raghava, *J. Polym. Sci. Polym. Phys. Ed.,* **25,** 1017 (1987).
6. K. Yamanaka and T. Inoue, *Polymer,* **30,** 662 (1989).
7. B. S. Kim, T. Chiba, and T. Inoue, *Polymer,* **34,** 2809 (1993).
8. B. S. Kim, T. Chiba, and T. Inoue, *Polymer,* **36,** 43, 67 (1995).
9. B. S. Kim and T. Inoue, *Polymer,* **36,** 1985 (1995).
10. B. S. Kim, *J. Appl. Polym. Sci.,* **65,** 85 (1997).
11. S. Shu and S. Konii, Jpn. Kokai Tokkyo Koho, JP 73,051,046 (1973).
12. B. M. Culbertson, O. Tiba, and M. L. Deviney, *34th Int. SAMPE Symp.,* 2483 (1989).
13. A. Matsumoto, K. Hasegawa, A. Fukuda, and K. Otsuki, *J. Appl. Polym. Sci.,* **44,** 205, 1547 (1992).
14. B. S. Kim, *Kor. Polym. J.,* **5,** 1 (1997).
15. J. Koberstein, T. P. Russel, and R. S. Stein, *J. Polym. Sci. Polym. Phys. Ed.,* **17,** 1719 (1979).
16. P. J. Plory, *Principles of Polymer Chemistry,* Cornell University Press, Ithaca, NY, 1953.
17. W. H. Stockmayer, *J. Chem. Phys.,* **11,** 45 (1943).
18. C. W. Macosko and D. R. Miller, *Macromolecules,* **9,** 199 (1976).